Cell Death and Ultrastructural Morphology of Femtosecond Laser–Assisted Anterior Capsulotomy

Wolfgang J. Mayer,[1,2] Oliver K. Klaproth,[1] Marko Ostovic,[1] Andreas Terfort,[3] Thalia Vavaleskou,[3] Fritz H. Hengerer,[1] and Thomas Kohnen[1]

[1]Department of Ophthalmology, Goethe-University, Frankfurt am Main, Germany
[2]Department of Ophthalmology, Ludwig-Maximilians-University, Munich, Germany
[3]Department of Biochemistry, Chemistry, and Pharmacy, Goethe-University, Frankfurt am Main, Germany

Correspondence: Thomas Kohnen, Department of Ophthalmology, Goethe-University, Theodor-Stern-Kai 7, 60590 Frankfurt am Main, Germany; kohnen@em.uni-frankfurt.de.

Submitted: September 26, 2013
Accepted: December 30, 2013

Citation: Mayer WJ, Klaproth OK, Ostovic M, et al. Cell death and ultrastructural morphology of femtosecond laser–assisted anterior capsulotomy. *Invest Ophthalmol Vis Sci*. 2014;55:893–898. DOI:10.1167/iovs.13-13343

Purpose. To evaluate cell death and ultrastructural effects on capsulotomy specimens derived from femtosecond laser–assisted cataract surgery.

Methods. In 26 eyes, an anterior capsulotomy was performed using a femtosecond laser. In 10 eyes (group 1), the laser-pulse energy was set to 15 μJ using a rigid curved interface and in another 10 eyes (group 2) to 5 μJ using a curved interface combined with a soft contact lens. The control group (6 eyes, group 3) underwent manual anterior capsulorhexis using forceps. All extracted capsule specimens underwent cell death analysis using the TUNEL kit, ultrastructural analyses using atomic force microscopy (AFM), and scanning electron microscopy (SEM). Counterstaining was performed with 4′,6-diamidino-2-phenylindol (DAPI) and hematoxylin-eosin (HE).

Results. Cell death was found in all capsule specimens along the cutting edge but was significantly more pronounced in group 1. DAPI and HE staining showed regular epithelial cell distribution with a demarcation line along the cutting edge of both laser groups, which was more pronounced in group 1. In AFM analysis, laser spot size in the femtosecond laser groups were in accordance with the preoperative planned size ($P < 0.01$). Cutting edges in SEM observations were smoother and more roundly shaped using 5 μJ (group 2).

Conclusions. Cutting edges of femtosecond laser–performed capsulotomies are precise and laser spot lesions are within planned size. Cell death reaction depends on the laser pulse energy settings and can be reduced to the level observed in a manual capsulorhexis.

Keywords: femtosecond laser, capsulotomy, capsulorhexis, laser energy, cell death, apoptosis, atomic force microscopy, scanning electron microscopy

A precise and well-performed capsulorhexis is crucial to perform an uncomplicated cataract extraction, intraocular lens implantation, and centration.[1–3] This main step in cataract surgery and refractive lens exchange surgery is commonly performed manually.

Femtosecond lasers are now changing how lens surgery is performed by becoming involved in the main steps of the surgical process: corneal incisions, capsulotomy, and lens fragmentation. Dick et al.[2] recently suggested a new terminology for opening the anterior lens capsule with a femtosecond laser: capsulotomy instead of capsulorhexis, as the femtosecond laser operates as a cutting knife by using focal photodisruption.

Recent studies have already demonstrated that femtosecond laser–performed capsulotomies allow repeatable and precise sizing and centration; furthermore, they improve the safety of hydrodissection, nuclear fragmentation, and cortical clean-up.[4–9] This maximizes the performance after implantation of intraocular lenses (IOL) with enhanced optical properties such as toric or multifocal IOL. On the other hand, histomorphological examinations have shown that femtosecond laser–performed capsulotomies show a prominent demarcation line with cell retraction along the cutting edge when exposed to increasing laser pulse energies.[10]

During capsulotomy, the anterior capsule is being injured and epithelial cell death is induced. This effect might be stronger with the assistance of femtosecond lasers.

Therefore, the purpose of this study was to investigate cell death reaction after anterior capsulotomy either performed by a femtosecond laser using different energy levels or manually by using forceps. Furthermore, laser spot lesions and cutting edge of all capsulotomy specimens were investigated on the ultrastructural level.

Methods

The experimental study was approved by the ethics committee of the Goethe-University, Frankfurt am Main, Germany, and was performed in accordance with the Declaration of Helsinki at the Department of Ophthalmology, Goethe-University.

In 26 eyes of 26 patients diagnosed with corticonuclear cataract formation anterior femtosecond laser–assisted capsulotomy ($n = 20$) or manual capsulorhexis ($n = 6$) using forceps was performed. In 10 eyes (group 1) that underwent femtosecond laser capsulotomy, the laser pulse energy was set to 15 μJ and applanation to the ocular surface was performed using a rigid curved interface. For another 10 eyes

TABLE. Laser Parameters for Each Procedure Step (Corneal Incisions, Anterior Capsulotomy, Lens Softening)

Parameters	Value
Corneal incisions	
Incision width, mm	2.2 or 2.4
Pulse energy, μJ	7.0
Spot separation, μm	4.0
Layer separation, μm	4.0
Capsulotomy	
Capsulotomy diameter, mm	5.0
Pulse energy, μJ (depending on the used interface)	5.0 or 15.0
Spot separation, μm	3.0
Layer separation, μm	3.0
Lens softening	
Chop diameter, mm	4.8
Cylinder diameter, mm	2.0
Number of Cuts/Cylinders	3/1
Pulse energy, μJ (depending on the used interface)	5.0 or 15.0
Spot separation, μm	10.0
Layer separation, μm	12.0

(group 2), the energy level was set to 5 μJ and a soft contact lens–based curved interface was used. Both interfaces use an applanation lens with a diameter of 10.8 mm and a curvature of 8.3 mm. The integrated optical coherence tomography (OCT) of the laser system was used to align treatment parameters.

Femtosecond Laser–Assisted Capsulotomy

The laser (LenSx; Alcon Laboratories, Inc., Fort Worth, TX) used in this study, is a femtosecond infrared laser with a repetition rate of 50 kHz, pulse width of 600 to 800 fs, and central laser wavelength of 1030 nm. Laser pulse energy setting in our trial was 15 μJ (group 1) or 5 μJ (group 2) with a spot separation size of 3 μm and layer separation of 3 μm for performing femtosecond laser–assisted anterior capsulotomy. Capsulotomy diameter was set to 5.0 mm and the anterior/posterior safety zone for laser treatment was ±300 μm. OCT parameters of the capsulotomy procedures and the treatment time were recorded. All treatment modalities for cataract surgery within the laser platform were carried out in all eyes by one experienced surgeon (TK)—i.e., corneal incisions, capsulotomy, and lens fragmentation (Table).

After the successful anterior capsule extraction, all the specimens from both groups were immediately fixed in formalin (4.5% paraformaldehyde in PBS, pH 7.4, freshly prepared) for 1 hour to further avoid additional mechanically induced apoptosis reaction. Afterward, the specimens were carefully placed on slides with the convex surface pointing down and underwent further analyses of cell death reaction and ultrastructure analyses using atomic force microscopy (AFM) and scanning electron microscopy (SEM).

Cell Death Analysis

The TUNEL assay preferentially labels DNA strand breaks generated during cell death.

For TUNEL analyses, a cell death kit (In situ cell death detection kit, fluorescein; Roche, Mannheim, Germany) was used in our experiments as previously described.[11] Briefly, anterior capsule specimens were dried at room temperature for 15 minutes after fixation and then rinsed in a balanced salt solution. Then, specimens were incubated with 0.1% Triton X-100 in 0.1% sodium citrate for 2 minutes on ice (2–8°C).

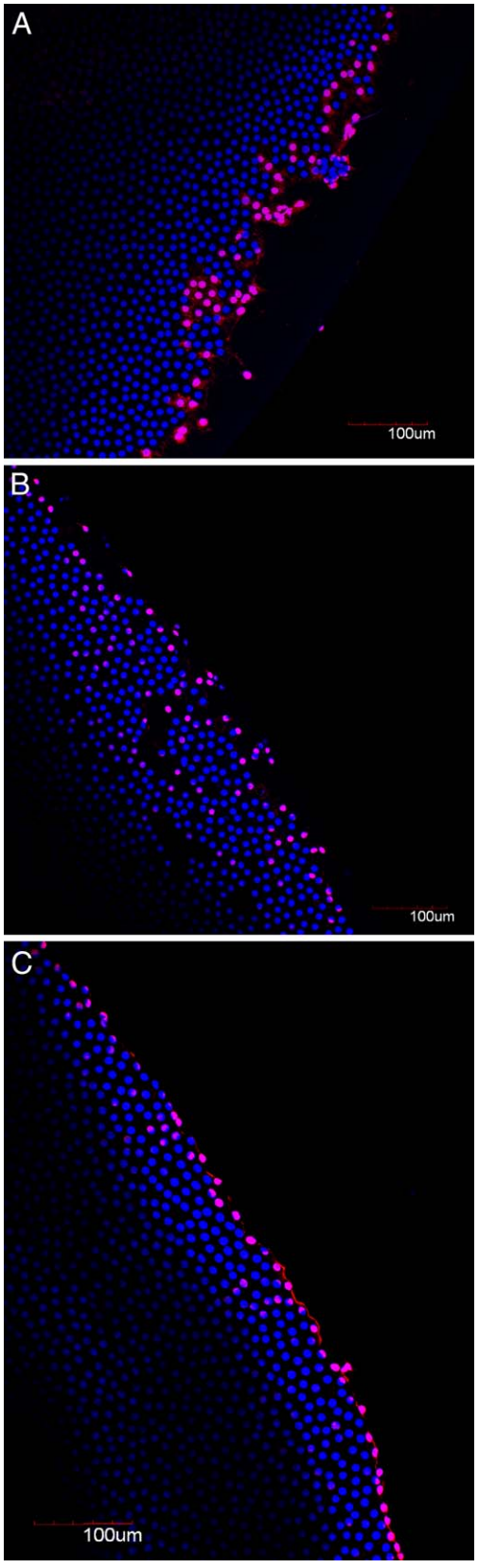

FIGURE 1. Distribution of TUNEL-positive cells (*red cells*) along the cutting edge in anterior capsulotomy specimens. (**A**) Group 1 (femtosecond laser, 15 μJ). (**B**) Group 2 (femtosecond laser, 5 μJ). (**C**) Group 3 (manual procedures). Counterstaining of nonspecific cells using DAPI technique (*blue cells*). Magnification: ×100.

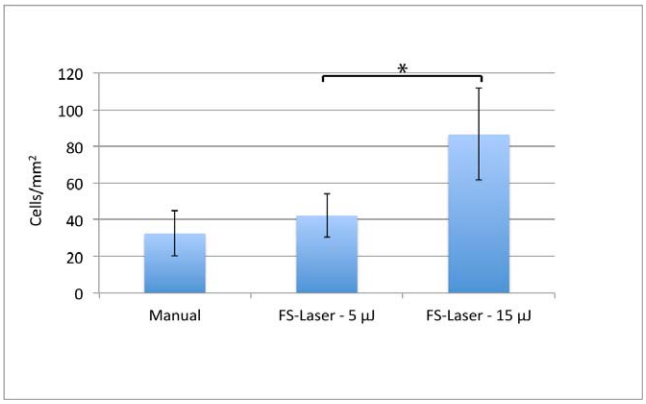

FIGURE 2. Quantification of TUNEL-positive cells in anterior capsulotomy specimens along the cutting edge using different treatment modalities. *Significant difference in cell death response, $P < 0.01$.

Afterwards, the slides were incubated with 50 µL of TUNEL reaction mixture for 1 hour at 37°C according to the manufacturer's protocol.

Specimen counterstaining for all the treatment groups was performed using either 4′,6-diamidino-2-phenylindol (DAPI) technique (Invitrogen Ltd., Paisley, Scotland) or standard hematoxylin-eosin (HE) staining to differentiate against dead cells. Afterward, all the probes were covered with fluorescent mounting medium (Vectashield; Vector Laboratories, Burlingame, CA).

A digital fluorescence microscope (FluoView 1000; Olympus Corporation, Tokyo, Japan) was used to analyze and obtain digital images. Each specimen was inspected over its entire area using total magnifications of ×50, ×100, and ×200. The expression of all the used assays was recorded. A software-controlled scanning grid (PicEd Cora; Jomesa Messsysteme GmbH, Munich, Germany) enabled the counting of positive stained cells. Three randomized regions along the cutting edge at 100 × 100 µm in size were selected and the mean cell counts were averaged (cells/mm²).

Atomic Force Microscopy (AFM)

Atomic force microscopy of the femtosecond laser–derived specimens was performed using an atomic force microscope (Veeco Instruments, Inc., Plainview, NY) after cell death analyses. Measurements of the specimens, fixed on slides, were performed in tapping mode at room temperature. The AFM operates by scanning a tip attached to the end of an oscillating cantilever across the sample surface. The cantilever is oscillated at or near its resonance frequency with amplitude ranging from 20 nm to 100 nm. The frequency of oscillation can be at or near the resonant frequency. The tip lightly "taps" on the sample surface during scanning, contacting the surface at the bottom of its swing. The feedback loop maintains constant oscillation amplitude. Calibration of the atomic force microscope was performed before each measurement session. Pyramidal, silicon nitride AFM cantilever tips (10-nm tip diameter, nominal spring constant 25–75 N/m, MLCT series, Bruker AFM Probes [Camarillo, CA]) were used to image all samples. All images were acquired at a scan rate of 0.3 to 0.8 Hz lines per second with a 256- × 256-pixel image definition. Image processing included flattening (first-third order) depending on the image. Image analysis was performed using the software from Veeco (Nanoscope 5.31r1). Laser spot size diameters were measured on three randomized cutting areas and cutting edges were visualized using a three-dimensional image reconstruction.

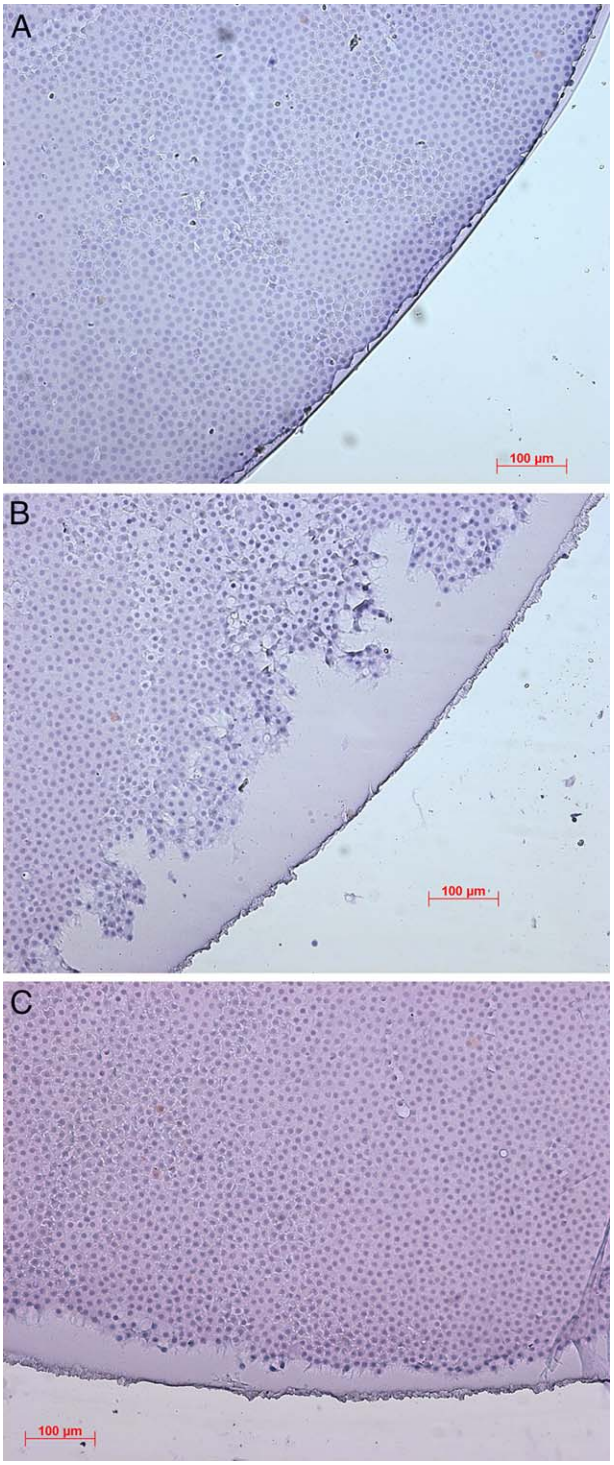

FIGURE 3. Morphological aspects of the cutting edge in manually performed capsulorhexis (**A**) compared with femtosecond laser-assisted capsulotomies (15 µJ [**B**], 5 µJ [**C**]) with irregularities of the cell configuration and partly destroyed nuclei in the peripheral part along the demarcation line. HE staining; magnification: ×100.

Scanning Electron Microscopy

Coating of the specimens for SEM was performed after AFM analysis with a thin layer of gold in a sputter chamber and examined with the scanning electron microscope at 20 keV beam energy. SEM images of the cutting edges in the

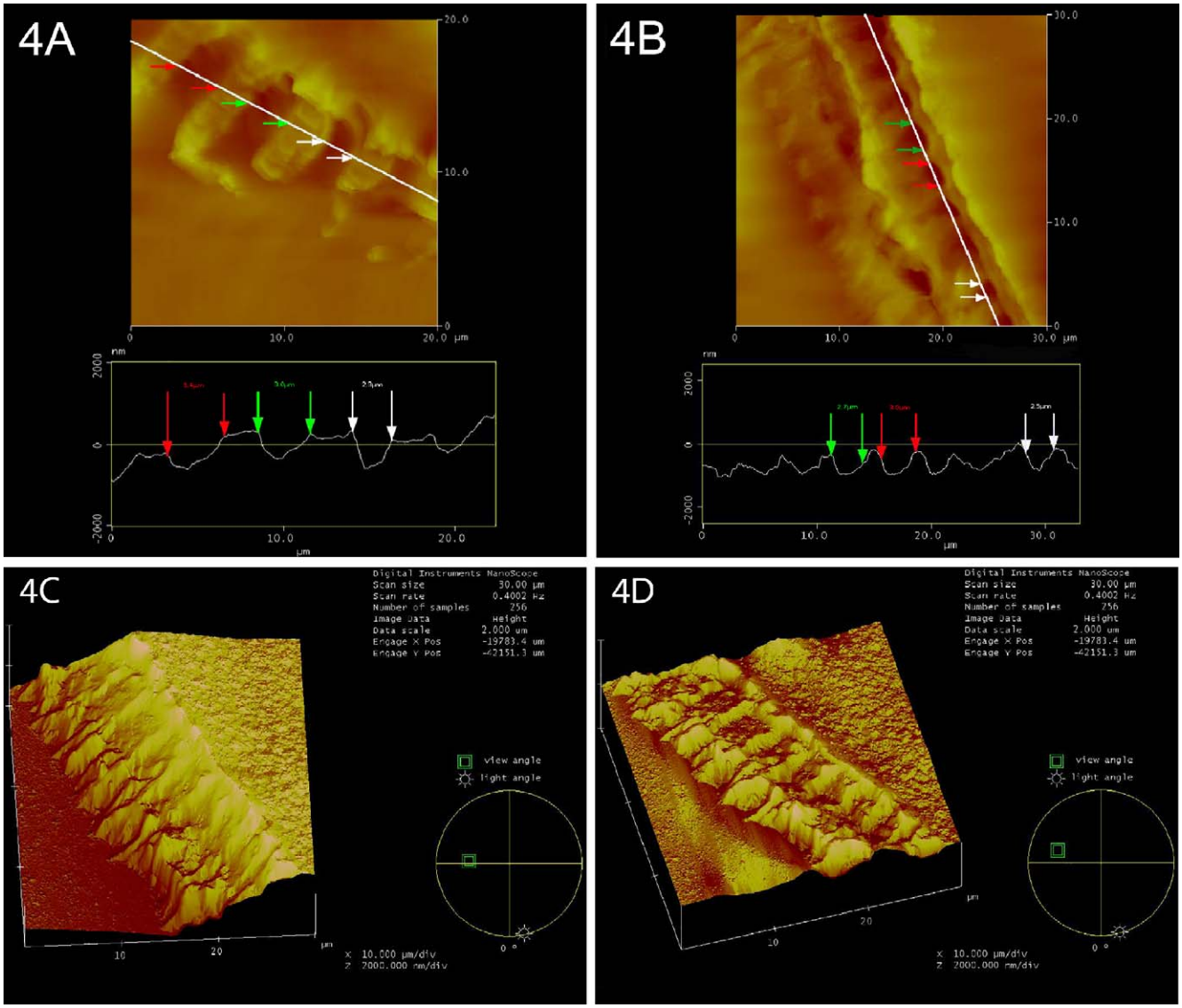

Figure 4. AFM of aligned femtosecond laser spots at the cutting edge. Mean spot size diameters (horizontal distance) in both laser groups were in accordance to the planned 3-µm laser spot separation configuration ($P < 0.01$; 15 µJ [**A**], 5 µJ [**B**]). Three-dimensional reconstruction of cutting edges showing a 2-step–like "valley and mountain" structure in both laser groups (15 µJ [**C**], 5 µJ [**D**]).

capsulotomy specimens from all the groups were captured with a commercial microscope (Amray 1920 ECO; SEMTech Solutions, Inc., Billerica, MA), with further focus on three random cutting edges from all the specimens.

Statistics

Data was evaluated by statistical software (SPSS version 21; IBM, Armonk, NY). A Student's *t*-test was used to compare the number and distribution of positive labelled cells in different lens capsule areas. The Wilcoxon test was used to compare data between groups. Variations were expressed as standard errors of the mean. A P value < 0.05 was considered to be significant.

Results

All the performed surgical treatments were uneventful and in all groups, a complete anterior lens capsule removal was possible. In the femtosecond laser groups, overall capsulotomy procedure duration was 3.0 ± 0.8 seconds in group 1 and 3.1 ± 0.9 seconds in group 2. OCT measurements of the anterior capsule procedures including the safety zone showed an anterior capsule treatment thickness of 293.26 ± 184.93 µm (group 1) and 268.10 ± 181.77 µm (group 2).

Cell Death

Cell death was detected in all groups mainly along the cutting edges. Comparing groups, the highest number of TUNEL-positive cells was found in the laser group using 15 µJ (group 1, Fig. 1A) followed by group 2 using 5 µJ (Fig. 1B) and group 3 (manual procedure, Fig. 1C). The ratio between the groups was 2.7 (15 µJ versus manual), 1.3 (5 µJ versus manual), and 2.0 between laser groups (Fig. 2). In the manual specimens, cell death was only found in the periphery along the cutting edge, whereas in femtosecond laser capsulotomies, cell death reaction was recorded along the demarcation line around laser spot areas with noticeable variance (Figs. 1A–C).

HE staining revealed a regular distribution of lens epithelial cells in the manual group and no cell demarcation area (group 3, Fig. 3A), whereas in group 1 and 2 irregularities of the cell configuration with partly destroyed nuclei were observed in the peripheral part along a demarcation line of the anterior capsule (Figs. 3B, 3C).

Atomic Force Microscopy

To evaluate laser spot size diameters, AFM was used in the femtosecond laser capsule specimens (group 1 and 2). Here we found mean spot size diameters of 3.1 ± 0.4 μm (horizontal distance, group 1) and of 2.9 ± 0.3 μm (horizontal distance, group 2), which is in accordance with the planned 3 μm laser layer separation configuration (Figs. 4A, 4B, $P < 0.01$). Cutting edges in both laser groups showed a regularly 2-step "valley and mountain" like structure along the cutting edge in a three-dimensional image reconstruction model (Figs. 4C, 4D).

Scanning Electron Microscopy

Compared with manual capsulotomies, both laser groups showed a "valley and mountain" like cutting edge in SEM observations. In higher magnifications, cutting edges were smoother and more roundly shaped using 5 μJ (group 2, Fig. 5A) compared with group 1 using 15 μJ that showed a more sawtooth-like cutting pattern (Fig. 5B).

Discussion

The present study demonstrates that human lens epithelial cells (LECs) undergo cell death after anterior lens capsule extraction during femtosecond laser–assisted cataract surgery. To our knowledge, this is the first study which compares femtosecond laser–assisted capsulotomies with manual performed continuous curvilinear capsulorhexis in this regard. Furthermore, using lower laser pulse energy levels, smoother cutting edges can be generated with reduced surrounding tissue affected, as previously described by our study group.[10]

Friedman et al.[7] demonstrated in a porcine model that femtosecond laser–produced capsulotomies were more precise, accurate, reproducible, and stronger than those created by the conventional manual technique. By using atomic force microscopy, it is possible to analyze the laser pulse effect on the capsule tissue. We found no significant difference in size of the applied laser spots between different laser pulse energy levels. Laser spots were arranged in a line and we observed only a small amount of laser spots straying. We presume that laser straying—as verified in the 2-step–like cutting edge structure in the three-dimensional AFM images—might be due to minimal torsional movements of the eye during treatment and is also affected by the applied interface as described by Talamo et al.[12]

We have already demonstrated that femtosecond laser–performed capsulotomies show an irregular cell pattern with destroyed nuclei of epithelial cells along the demarcation line of capsule specimens.[10,13] This may have an influence on posterior capsule opacification. Lens epithelial cells exist in a single layer and form the lens capsule, which is composed mainly of type IV collagen.

Posterior capsule opacification (PCO) is one of the main causes of visual acuity deterioration after cataract surgery and is caused by LECs,[14–17] which reside in the capsular bag and undergo proliferation and metaplasia.[14,18,19] Recent studies have investigated the behavior of human LECs during healing after cataract surgery and found that LECs proliferate on the inner surface of the residual lens capsule and accumulate extracellular matrix.[14–16,20]

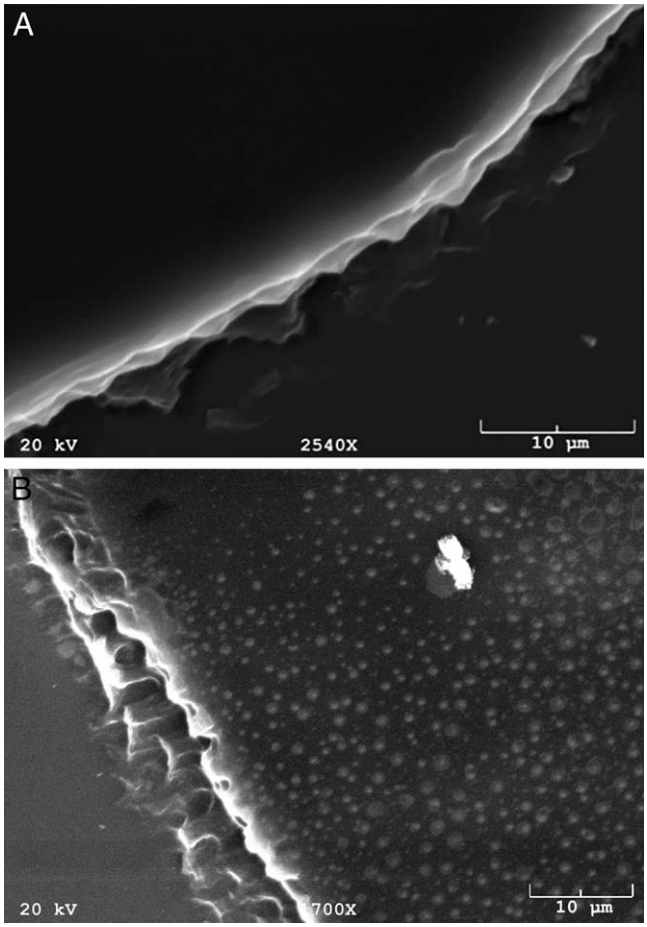

Figure 5. Scanning electron microscopy of cutting edges in femtosecond laser–assisted capsulotomy with a smoother cutting line using 5 μJ (**A**) compared with 15 μJ (**B**). Magnifications: ×2540 (**A**) and ×1700 (**B**).

The present study indicates that these cells are fed to the death after anterior capsulotomy and were distributed in all of the analyzed specimens along the cutting edges in the monolayered epithelium beneath the anterior capsule. In the control group, only a few dead cells were identified, which might be induced due to mechanical injury while using forceps for anterior capsule extraction. Apoptosis occurs in the course of embryonic development, in the maintenance of tissue homeostasis, and in response to infections or toxic damage.[21] In the femtosecond laser groups, cell death of LECs is upregulated, which we attribute to the high laser pulse energy. Therefore, LEC proliferation is inhibited and might therefore prevent capsular bag opacification. Moreover, when using higher energy pulse levels in femtosecond laser procedures, this effect might be increased, but the effect on cutting edge irregularities should then be taken into account.

Further studies and long-term follow-up examinations are needed to observe if femtosecond laser–performed capsulotomies might have an influence on capsule opacification and capsule stiffness since the demand for optimized intraocular lens models and their centering in the capsular bag together with the patient's claim is steadily increasing.

Investigative Ophthalmology & Visual Science

Acknowledgments

We thank Sabine Albrecht and Ralf Lieberz from the Department of Pathology, Goethe-University for assistance in sample preparation and staining techniques. The authors alone are responsible for the content and writing of the paper.

Disclosure: **W.J. Mayer**, Allergan (C, R), Carl Zeiss Meditec (C); **O.K. Klaproth**, Alcon (R), Oculus (R), Rayner (R), Carl Zeiss Meditec (R), RTI-HS (C); **M. Ostovic**, None; **A. Terfort**, None; **T. Vavaleskou**, None; **F.H. Hengerer**, None; **T. Kohnen**, Thieme Compliance (C), Alcon (C, R), Carl Zeiss Meditec (C, R), Rayner (C, R), Schwind (C, R), Abbott (R), B&L (R), Neoptics (R)

References

1. Aslan L, Aksoy A, Aslankurt M, Ozdemir M. Lens capsule-related problems in patients undergoing phacoemulsification surgery. *Clin Ophthalmol*. 2013;7:511–514.
2. Dick HB, Gerste RD, Schultz T, Waring GO III. Capsulotomy or capsulorhexis in femtosecond laser-assisted cataract surgery? *J Cataract Refract Surg*. 2013;39:1442.
3. Kranitz K, Takacs A, Mihaltz K, Kovacs I, Knorz MC, Nagy ZZ. Femtosecond laser capsulotomy and manual continuous curvilinear capsulorrhexis parameters and their effects on intraocular lens centration. *J Refract Surg*. 2011;27:558–563.
4. Abell RG, Kerr NM, Vote BJ. Femtosecond laser-assisted cataract surgery compared with conventional cataract surgery. *Clin Experiment Ophthalmol*. 2013;41:455–462.
5. Conrad-Hengerer I, Al Juburi M, Schultz T, Hengerer FH, Dick HB. Corneal endothelial cell loss and corneal thickness in conventional compared with femtosecond laser-assisted cataract surgery: three-month follow-up. *J Cataract Refract Surg*. 2013;39:1307–1313.
6. Conrad-Hengerer I, Hengerer FH, Schultz T, Dick HB. Effect of femtosecond laser fragmentation on effective phacoemulsification time in cataract surgery. *J Refract Surg*. 2012;28:879–883.
7. Friedman NJ, Palanker DV, Schuele G, et al. Femtosecond laser capsulotomy. *J Cataract Refract Surg*. 2011;37:1189–1198.
8. Nagy ZZ. Advanced technology IOLs in cataract surgery: pearls for successful femtosecond cataract surgery. *Int Ophthalmol Clin*. 2012;52:103–114.
9. Roberts TV, Lawless M, Bali SJ, Hodge C, Sutton G. Surgical outcomes and safety of femtosecond laser cataract surgery: a prospective study of 1500 consecutive cases. *Ophthalmology*. 2013;120:227–233.
10. Ostovic M, Klaproth OK, Hengerer FH, Mayer WJ, Kohnen T. Light microscopy and scanning electron microscopy analysis of rigid curved interface femtosecond laser-assisted and manual anterior capsulotomy. *J Cataract Refract Surg*. 2013;39:1587–1592.
11. Mayer WJ, Grueterich M, Wolf AH, et al. Corneal cell response after flap creation using a mechanical microkeratome or a 200 kHz femtosecond laser. *J Cataract Refract Surg*. 2013;39:1088–1092.
12. Talamo JH, Gooding P, Angeley D, et al. Optical patient interface in femtosecond laser-assisted cataract surgery: contact corneal applanation versus liquid immersion. *J Cataract Refract Surg*. 2013;39:501–510.
13. Kohnen T, Klaproth OK, Ostovic M, Hengerer FH, Mayer WJ. Morphological changes in the edge structures following femtosecond laser capsulotomy with varied patient interfaces and different energy settings. *Graefes Arch Clin Exp Ophthalmol*. 2014;252:293–298.
14. Bertelmann E, Kojetinsky C. Posterior capsule opacification and anterior capsule opacification. *Curr Opin Ophthalmol*. 2001;12:35–40.
15. Rakic JM, Galand A, Vrensen GF. Lens epithelial cell proliferation in human posterior capsule opacification specimens. *Exp Eye Res*. 2000;71:489–494.
16. Sacu S, Menapace R, Findl O. Effect of optic material and haptic design on anterior capsule opacification and capsulorrhexis contraction. *Am J Ophthalmol*. 2006;141:488–493.
17. Werner L, Pandey SK, Apple DJ, Escobar-Gomez M, McLendon L, Macky TA. Anterior capsule opacification: correlation of pathologic findings with clinical sequelae. *Ophthalmology*. 2001;108:1675–1681.
18. Ohara K, Itakura K, Ibaraki N. Anterior capsule opacification: a cell culture model. *Acta Ophthalmol Suppl*. 1992;29–33.
19. Werner L, Pandey SK, Escobar-Gomez M, Visessook N, Peng Q, Apple DJ. Anterior capsule opacification: a histopathological study comparing different IOL styles. *Ophthalmology*. 2000;107:463–471.
20. Wejde G, Kugelberg M, Zetterstrom C. Position of anterior capsulorhexis and posterior capsule opacification. *Acta Ophthalmol Scand*. 2004;82:531–534.
21. Hetts SW. To die or not to die: an overview of apoptosis and its role in disease. *JAMA*. 1998;279:300–307.

Investigative Ophthalmology & Visual Science